Journal of Catalysis 276 (2010) iii–viii

Contents lists available at ScienceDirect

Journal of Catalysis

journal homepage: www.elsevier.com/locate/jcat

Journal of Catalysis Vol. 276, Issue 1, 2010

Contents

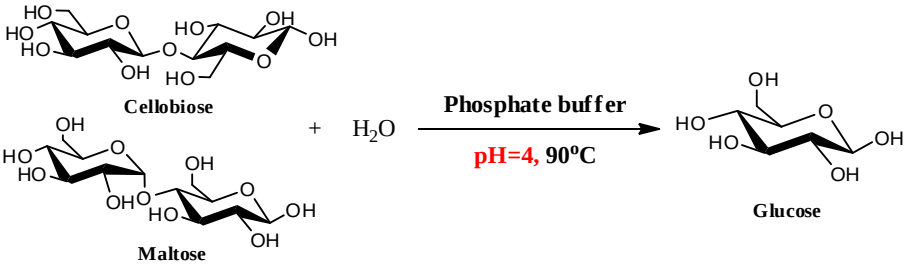

Glycosidic bond hydrolysis in both cellobiose and maltose proceeds under unexpectedly mild conditions when using simple phosphate salts as catalyst.

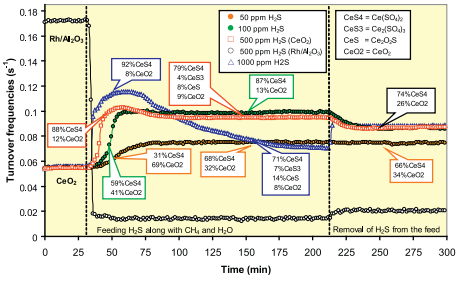

Unlike conventional metallic-based catalysts, the presence of poisonous H_2S gas (with appropriate content) increases the steam reforming rate of CeO_2-based catalysts, which is related to the formation of $Ce(SO_4)_2$ phase during the reaction.

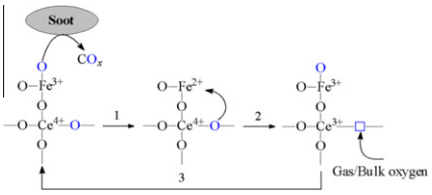

The densities of active oxygen sites and turnover frequencies for soot combustion on Fe-doped CeO_2 mixed oxides are determined by isothermal anaerobic titrations with soot as the probe molecule.

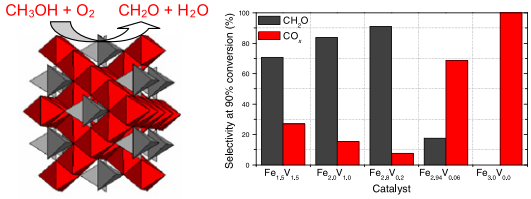

Cation vacant spinel phases with V-sites surrounded by Fe (V–O–Fe) are stable, active, selective and non-volatile in methanol oxidation to formaldehyde.

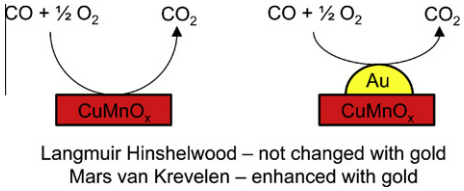

TAP studies of the CO oxidation reactions over $CuMnO_X$ (Hopcalite) catalysts has revealed that the increased activity on doping with gold is due to promotion of the Mars van Krevelen mechanism with little change in the activity associated with the Langmuir-Hinshelwood mechanism.

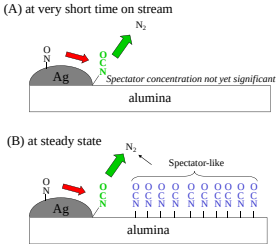

Examination of the H_2-assisted Selective Catalytic Reduction of NO_X with octane over a Ag/Al_2O_3 catalyst using fast transient cycling switching of H_2, monitored by DRIFTS and mass spectrometry, suggests that *some* of the isocyanate species could be important intermediates in this reaction.

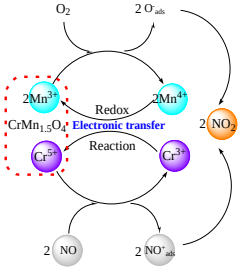

Impressive activity for low-temperature SCR of NO_x is achieved on novel catalysts containing $CrMn_{1.5}O_4$ phase, which provides catalytically active sites due to facilitated electron transfer between Cr and Mn.

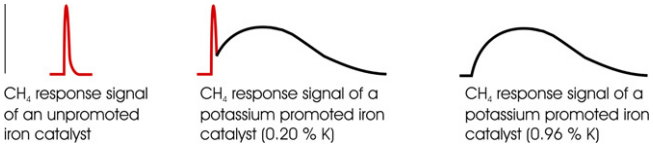

CH_4 formation over unpromoted and potassium-promoted iron catalysts applied in Fischer–Tropsch synthesis was studied via hydrogenation of CO during pulse experiments. The presence of potassium influences CH_4 formation by blocking the fast formation channel at least partially and establishing a new and slower reaction pathway.

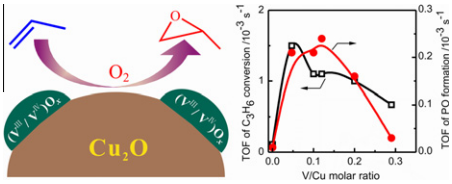

Modification of unsupported copper by vanadium significantly enhances its catalytic activity for propylene epoxidation. Cu^I with cooperation of vanadium species at lower valance states is responsible for propylene oxide formation.

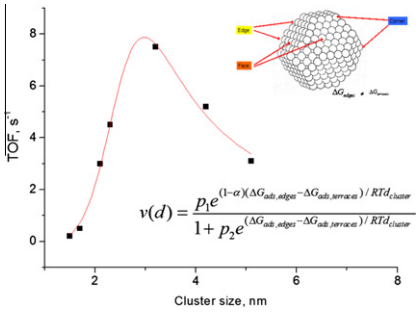

The impact of nanoparticle size effects in heterogeneous catalytic kinetics over supported metal catalysts is discussed taking into account different activities of edges and terraces.

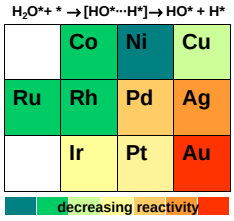

Water dissociation on regular, stepped and folded transition metal surfaces follows a BEP relationship. In addition, the adsorption energy of atomic oxygen on a given metallic surface provides an excellent descriptor of the activation energy thus allowing the screening of a large number of metallic and bimetallic systems in a simple way.

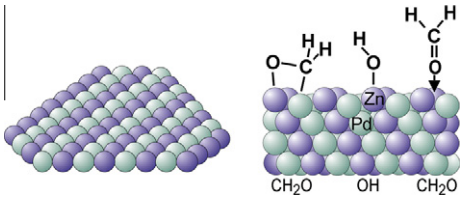

The bifunctional sites for methanol reforming on a multi- and monolayer Pd–Zn surface are structurally different, despite identical surface composition. The multilayer alloy activates water for reaction to CO_2 and H_2.

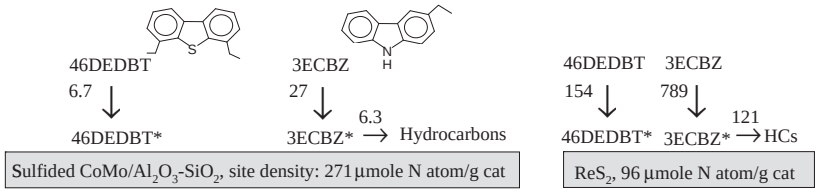

Shown here are adsorption constants for 4,6-diethyldibenzothiophene (46DEDBT) and 3-ethylcarbazole (3EBZ) and hydrodenitrogenation rate constants on sulfided $CoMo/Al_2O_3$–SiO_2 and ReS_2. ReS_2 is more active for HDN; its HDS activity is less resilient to 3ECBZ inhibition.

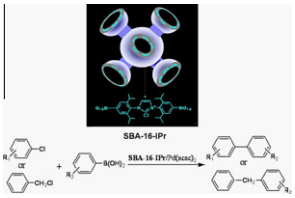

New mesoporous hybrid materials with a built-in N-heterocyclic carbene in the framework were synthesized. Such materials are active and recyclable for Suzuki–Miyaura coupling of challenging aryl/benzylic chlorides.

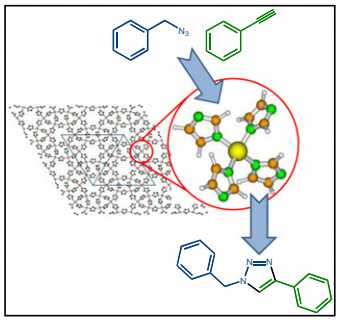

Copper-containing metal organic frameworks are highly active and fully regioselective heterogeneous "click" catalysts, with performances comparable to homogeneous Cu catalysts.

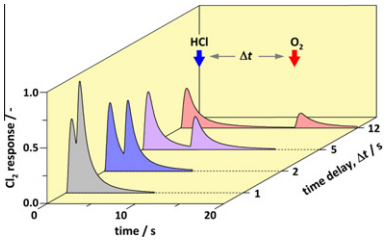

Temporal Analysis of Products (TAP) reactor studies improve the mechanistic understanding of the gas-phase HCl oxidation to Cl_2 (Deacon process) over RuO_2-based catalysts.

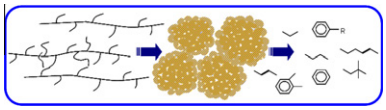

Hierarchical nanocrystalline ZSM-5 materials, prepared by a seed silanization method, showed a remarkable enhancement of the catalytic activity in the cracking of polyolefins compared to hierarchical ZSM-5 samples synthesized by a low-temperature procedure, the differences being especially pronounced for the case of waste polyethylene conversion.

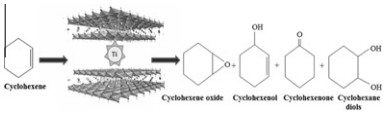

The solvent-free epoxidation reaction of cyclohexene using Ti–Schiff base complex-immobilized LDH will help experimentalist to achieve greener and most sustainable process.

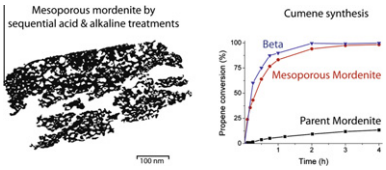

Commercially available mordenite was subjected to post-synthesis treatments. Sequential acid and alkaline treatments were found to be most effective to obtain mesoporous mordenite and visualized with electron tomography. Mesoporous mordenite was close in activity to zeolite beta for the production of cumene, with superior selectivity toward the undesired *n*-propylbenzene.

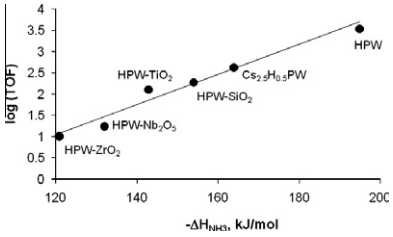

The strength of acid sites of supported $H_3PW_{12}O_{40}$ (HPW) catalysts (enthalpy of NH_3 adsorption) is weaker, and their catalytic activity in isopropanol dehydration (TOF) is lower than those of the standard unsupported catalysts (bulk HPW and $Cs_{2.5}H_{0.5}PW_{12}O_{40}$); they decrease in the order of supports: SiO_2 > TiO_2 > Nb_2O_5 > ZrO_2 (all catalysts calcined at 300 °C).

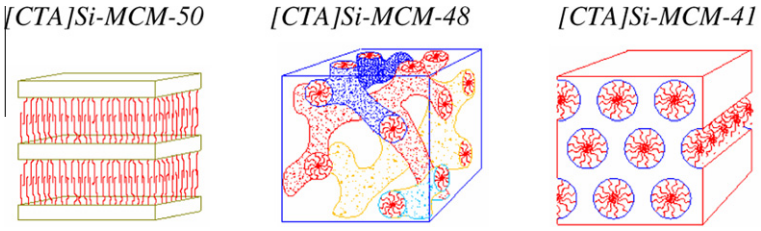

Template-containing molecular sieves such as [CTA]Si–MCM-48 were shown to possess very weak basic sites by calorimetry, however the CO_2 adsorption isotherms are totally reversible. Their catalytic activities in transesterification are comparable to that of strong inorganic bases.